

Ultrahigh-Gradient Acceleration of Injected Electrons by Laser-Excited Relativistic Electron Plasma Waves

C. E. Clayton, K. A. Marsh, A. Dyson, M. Everett, A. Lal, W. P. Leemans,^(a) R. Williams,^(b) and C. Joshi

Department of Electrical Engineering, University of California, Los Angeles, California 90024

(Received 14 September 1992)

High-gradient acceleration of externally injected 2.1-MeV electrons by a laser beat wave driven relativistic plasma wave has been demonstrated for the first time. Electrons with energies up to the detection limit of 9.1 MeV were detected when such a plasma wave was resonantly excited using a two-frequency laser. This implies a gradient of 0.7 GeV/m, corresponding to a plasma-wave amplitude of more than 8%. The electron signal was below detection threshold without injection or when the laser was operated on a single frequency.

PACS numbers: 52.35.Mw, 52.40.Nk, 52.75.Di

Recently there has been a resurgence of interest in collective particle acceleration techniques using waves in plasmas because of their potential for ultrahigh \sim GeV/m gradient acceleration of particles [1]. In one such scheme, known as the plasma beat wave accelerator [2], two copropagating laser beams with frequencies and wave numbers ω_1, k_1 and ω_2, k_2 resonantly drive a plasma wave with frequency $\omega_p = \omega_2 - \omega_1$ and wave number $k_p = k_2 - k_1$. The phase velocity $v_\phi = \omega_p/k_p$ of this relativistic plasma wave is nearly the speed of light c if $\omega_1 \approx \omega_2 \gg \omega_p$. The longitudinal electric field associated with such a wave is given by $\epsilon n_0^{1/2}$ V/cm, where ϵ is the density modulation n_1/n_0 and n_0 is the plasma electron density in cm^{-3} . Thus for $n_1/n_0 = 0.1$ and $10^{15} < n_0 < 10^{17} \text{ cm}^{-3}$, accelerating fields of $\approx 0.3 < E < 3$ GeV/m are possible. Experiments around the world have reported beat excitation of relativistic plasma waves using CO_2 [3,4] and Nd:glass lasers [5]. However, no conclusive demonstration of acceleration of externally injected electrons has been reported. If practical, such an accelerator could have an impact on future high-energy linear colliders, compact sources of tunable x rays for materials and biological studies, and medical applications. In this Letter, we demonstrate for the first time such ultrahigh-gradient acceleration of externally injected electrons by laser beat wave excited relativistic electron plasma waves.

The experimental setup is shown schematically in Fig. 1. The CO_2 laser system [6] produced a two-frequency laser beam with 60 ± 10 J at wavelength $\lambda_1 = 10.59 \mu\text{m}$ and 10 ± 5 J at $\lambda_2 = 10.29 \mu\text{m}$. The resonant density is thus $n_0 = 8.6 \times 10^{15} \text{ cm}^{-3}$. The laser pulse had an approximately linear rise time of 150 ps and 300 ps FWHM. It was focused with an $f/11.5$ off-axis parabolic mirror to a nearly diffraction-limited spot size of $300 \mu\text{m}$ diameter, resulting in peak normalized quiver velocities $a_{1,2} = eE_{1,2}/m\omega_{1,2}c = 0.17$ and 0.07, respectively. Here $E_{1,2}$ are the electric fields of the two laser beams. The vacuum chamber contained a static fill of hydrogen gas with fill pressure in the range 110–200 mTorr. The plasma, produced by tunnel ionization of the gas [7], was im-

aged onto a charge-coupled-device (CCD) camera. The images show the plasma existing over more than 20 mm along the laser beam with a fully ionized core emitting uniform brightness of visible radiation that is about 10 mm in length. The full length at half the peak intensity of the focused beam (twice the Rayleigh length z_R) was measured to be ≈ 16 mm. The laser has sufficient intensity to fully ionize the hydrogen at best focus by around 25 ps into the rising edge of the pulse and fully ionize over more than 12 mm on either side of best focus by the peak of the pulse [7].

The source of electrons for injection was a 9.3-GHz rf linac producing a train of 20-ps-long micropulses separated by 110 ps within a 5-ns macropulse envelope [8]. The average macropulse current where the plasma wave and the electrons overlap was 15 mA and the spot size of the $f/10$ -focused electrons was $\approx 250 \mu\text{m}$ FWHM. These electrons had an injection energy of 2.1 MeV with an energy spread of 5% FWHM. The laser and the electron macropulse were synchronized to ± 100 ps. A one-

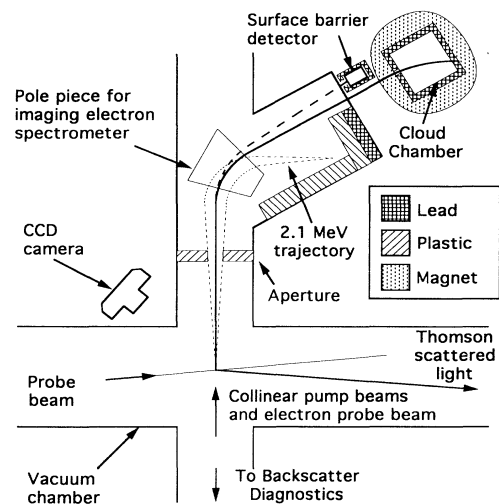


FIG. 1. Schematic of the experimental arrangement.

dimensional fluid model which includes tunnel ionization and relativistic detuning shows that the plasma-wave lifetime [9] is about 70 ps FWHM. Thus, the probability that a single microbunch will interact with the plasma wave is approximately 60%. Therefore, not all two-frequency laser shots should produce accelerated electrons. As a single microbunch overlaps with about 17 plasma wavelengths ($\lambda_p = 360 \mu\text{m}$), the energy spectrum of the accelerated electrons will have a continuous distribution up to some maximum energy. In the experiment the electrons entered a variable field imaging electron spectrometer [9] with an $f/8$ acceptance cone. The maximum magnetic field of the spectrometer only allows electrons up to 9.1 ± 0.15 MeV to be detected. The unaccelerated electrons were dumped onto low-density plastic as shown in Fig. 1. Lead shielding was used to reduce the flux of background x rays reaching the electron detectors, limiting the noise levels to a value negligibly small compared to the signal levels ultimately obtained. Upon exiting the vacuum chamber through a 25- μm -thick Mylar window, the accelerated electrons were detected using either one or more silicon surface barrier detectors (SBD) or by recording the tracks the electrons produced in a cloud chamber. The SBDs had a 600- μm -thick copper window which absorbed x rays to reduce the noise but was "transparent" to energetic electrons with greater than 3 MeV energy. Along with a charge-sensitive preamplifier, each SBD produces about 20 mV per electron in the 1–10-MeV energy range. The preamplifier saturates at ≈ 2.5 V thus limiting the number of detectable electrons to about 125. The cloud chamber used supersaturated methanol vapor in 1 atm of air to form visible tracks as electrons ionize the molecules along their path. In our experiment the electrons entered the cloud chamber through a 6- μm -thick Mylar window placed over a 3-mm-diam aperture in lead which shielded the cloud chamber from x rays. The electron tracks were recorded using a CCD camera. A uniform 260-G magnetic field was applied to the cloud chamber from coils wound around the lead shielding. This gave an independent confirmation of the electron energy from the radius of curvature of the electron tracks. At low electron fluxes individual electron tracks were counted, while at high fluxes the brightness of the cloud chamber image was calibrated (with the 2.1-MeV injector beam) and was shown to vary approximately linearly with the flux of electrons up to about 400 electrons/ mm^2 .

The collective oscillations of the plasma were probed with optical diagnostics: Thomson scattering and back-scattered incident laser light. These do not probe the beat wave excited relativistic plasma wave (fast wave) directly, but rather its mode-coupled daughter waves [10]. These quasimodes arise at approximately $\pm 2k_1$ due to coupling of the fast wave with the ion acoustic wave at $2k_1$ from stimulated Brillouin scattering. In Thomson scattering, a frequency-doubled YAG probe beam of 5 ns duration was transversely focused to a 50-

μm -diam spot within the 10-mm core of the plasma. The geometry was chosen to k match to waves with $k = \pm (2.0 \pm 0.5)k_1$. Thus, in addition to mode-coupled waves, the diagnostic also probed density fluctuations caused by stimulated Compton (SCS) [11] and Brillouin (SBS) [12] scattering. The scattered light was sent to a spectrograph and streak-camera combination with a 0.5- \AA wavelength and 25-ps time resolution. For backscatter, the entire cone of backscattered light was sampled with a beam splitter and sent to a spectrograph where the time-integrated spectrum was captured on a frame-grabbed pyroelectric camera.

During the course of this experiment we carried out the following null tests: First, no energetic electrons were detected when the laser and the electron beam were simultaneously fired into an evacuated chamber (no plasma). Second, no energetic electrons were observed when none were injected into plasmas produced by either single- or dual-frequency beams in contrast to recent Osaka experiments [4]. Therefore, there is no detectable contribution to the observed signal due to self-trapping of the background plasma electrons [13] in excited plasma oscillations. Third, with single-frequency illumination, no acceleration of electrons was observed even with injection of 2.1-MeV electrons. This implies that with dual-frequency illumination and injection, accelerating fields associated with waves generated by Raman forward scattering have a negligible contribution to the observed signal [14].

In our experiments, injected electrons were seen to gain energy only when a two-frequency laser beam was fired in a static gas over a narrow range of pressures. Figure 2(a) shows tracks from a shot for which the plasma density was nearly resonant (143 mTorr of H_2). For this laser shot the electron spectrometer was set to direct 5.2-MeV electrons into the cloud chamber and 5.9-MeV electrons into the SBD. The solid curves superimposed on Fig. 2(a) represent the calculated trajectories of 5.2-MeV electrons. The calculated and observed trajectories match extremely well, confirming that the electrons have gained energy from the beat wave interaction. The SBD signal corresponding to this shot was 360 mV or about 18 electrons (assuming SBD sensitivity of ≈ 20 mV/electron) in approximately the same solid angle. This agrees closely with the number of tracks seen in Fig. 2(a).

The experiment was repeated over a range of fill pressures with the electron spectrometer field set to observe various energies. The data are summarized in Fig. 2(b). We have previously shown that at these laser intensities, fully ionized plasmas are formed up to a plasma density $n_e \leq 2 \times 10^{16} \text{ cm}^{-3}$. Above this, density refractive effects become important [15]. Therefore, the desired density up to this limit can be obtained by changing the neutral gas pressure. The calculated pressure range over which a 4% amplitude or greater wave is expected is 126–138 mTorr with the optimum pressure [2] being 136 mTorr. Figure 2(b) shows that the signals are essentially in the noise

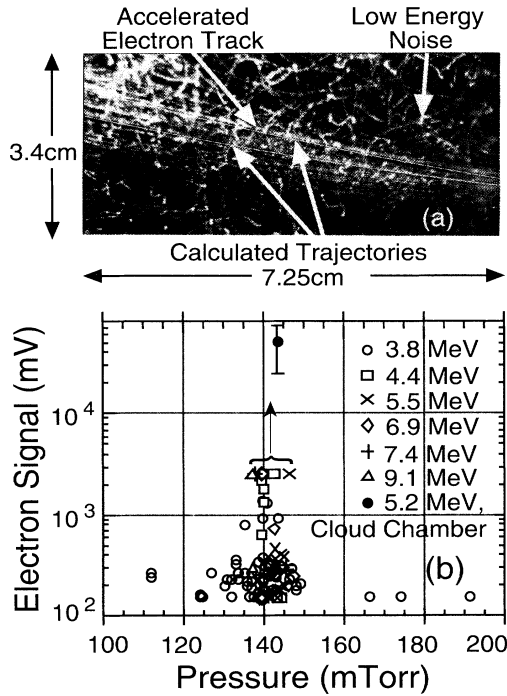


FIG. 2. (a) Electron trajectories in the cloud chamber with the magnetic field. The entrance aperture is located 6 cm to the right of this image. The superimposed curves represent theoretical trajectories for 5.2-MeV electrons. (b) Summary plot showing the electron signal on SBD obtained at various energies vs fill pressure. The one solid symbol is from cloud chamber data converted into units of equivalent SBD signal in mV. The mean noise level [9] was about 150 mV.

below 135 mTorr rising rapidly around 140 mTorr. However, there are not enough shots above 148 mTorr to confirm the exact location of the peak of the electron signal. The data points bracketed with an arrow indicate that on these shots the SBD signals were saturated. Thus these data points are indicative of the lower bound of the electron signal. However, the experiment appears to work best with about 5–10 mTorr higher pressure than the expected optimum. This may be a result of hydrodynamic motion of the hydrogen plasma which could lower the density by (5–10)% during the 70–100-ps growth time of the plasma wave. We have observed electrons with energies up to 9.1 MeV. Thus some electrons gained at least 7 MeV in traversing the roughly 1-cm-long plasma wave implying an accelerating gradient of more than 0.7 GeV/m which corresponds to a wave amplitude of at least 8%. A preliminary estimate of the number of accelerated electrons [9] indicates that in the energy range 5–9 MeV, roughly 3×10^4 electrons were accelerated (about 1% of the available electrons). A better estimate based on the single-shot measurement of the complete spectrum of the accelerated electrons is currently under way.

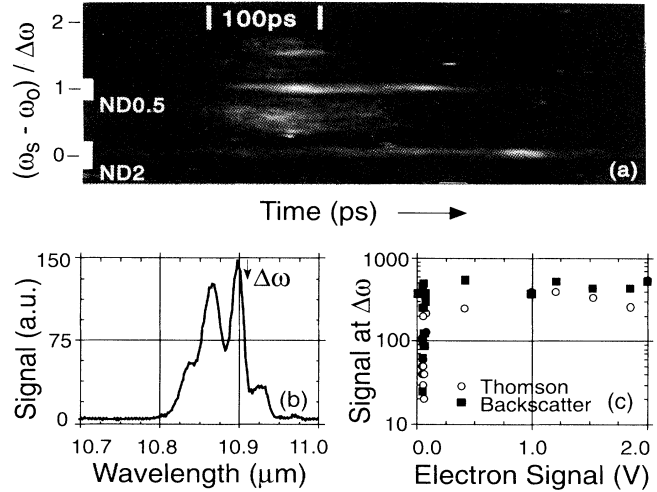


FIG. 3. (a) A streak image showing the time evolution of the Thomson scattered spectrum from modes near $2k_1$. The white boxes on the left indicate the location of neutral density attenuators to limit the signal at zero frequency shift (stray light and scattering from SBD ion wave) and at the plasma-wave frequency. (b) Typical data from the time-integrated backscatter spectrometer. The arrow shows the location for an exact $\Delta\omega$ shift of the 10.59- μm pump. (c) Correlation of the intensity of the first burst of Thomson scattered light at $(\omega_s - \omega_0)/\Delta\omega = 1$ and the backscattered light near $\Delta\omega(10.9 \mu\text{m})$ vs SBD electron signal for one set of data.

The measured electron signals were correlated with optical diagnostics to further confirm that the acceleration observed was associated with the relativistic plasma waves. The time-resolved Thomson scattered spectrum is shown in Fig. 3(a). It shows a broad band of scattered frequencies in the range $0 < (\omega_s - \omega_0)/\Delta\omega < 1.5$ which are due to SCS [15]. Here, ω_s and ω_0 are the scattered and incident frequencies of the Thomson probe, respectively, and $\Delta\omega \equiv \omega_2 - \omega_1$ is the beat frequency. There is in addition a narrower but much more intense feature at a frequency shift corresponding to $\Delta\omega$. This feature generally shows two temporal bursts. The first has a typical growth time of 50–70 ps and is thought to be due to the mode coupling of the relativistic plasma wave [10] from the still-growing ion acoustic wave. As expected, the strongest electron signals were observed on shots when the first burst at $\omega_s - \omega_0 = \Delta\omega$ was intense while SCS was still occurring. This is shown in Fig. 3(c). Not all laser shots with a strong burst at $\Delta\omega$ produced electron signals because of the 60% probability of the synchronization of the electrons and the plasma wave mentioned earlier. The second peak, which persists after SCS is over, is thought to arise from counterpropagating optical mixing which excites a slow phase velocity plasma wave. Such a wave cannot accelerate relativistic electrons significantly.

The backscatter spectrum, Fig. 3(b), also shows a feature shifted by $\approx \Delta\omega$ when a two-frequency laser is

used but at roughly a 3.5% less frequency shift than $\Delta\omega$. As with the Thomson diagnostic, strongest electron signals were observed when the feature at $\approx 10.9 \mu\text{m}$ was relatively intense [see Fig. 3(c)]. Our models for the Thomson scattering and backscattering [10] state that the scattered signals are essentially proportional to the intensity of the relativistic plasma wave and thus these signals represent an independent confirmation that the plasma wave does indeed exist. The correlation of the electron signal with strong scattering signals in the Thomson and the backscattering spectra further supports the notion that the electrons are accelerated by the relativistic plasma wave excited by collinear optical mixing. We should note that, like the electron signals, these optical signals were not observed away from the resonant pressure of 143 mTorr.

Finally, we have estimated the relativistic plasma-wave amplitudes from observed Thomson scattering harmonic components [16] (not shown) and from mode-coupling theory [10]. These suggest that waves of amplitude $n_1/n_0 \sim (15-30)\%$ were excited at the point probed by Thomson scattering. This is consistent with the maximum possible wave amplitude of about 37% for our pump strength, limited by relativistic saturation [17] predicted by the 1D model. The actual saturation amplitude may be lower than the ideal theoretical saturation amplitude due to hydrodynamic expansion of the plasma. Mode coupling, although it occurs, does not severely drain the energy from the plasma wave because of the small ion wave amplitudes, and the modulational instability is similarly unimportant because the plasma-wave growth occurs in less than 3 ion plasma periods.

We have carried out 3D particle trajectory simulations, which include finite emittance effects, based on the lower bound estimate of the maximum wave amplitude (E_{max}) inferred from the Thomson scattering diagnostic [18]. These suggest that for a plasma-wave envelope given by $E(z) = E_{\text{max}}/(1+z^2/z_R^2)$, electrons up to 20 MeV might be observable for a 15% wave [19].

In conclusion, high-gradient acceleration of externally injected electrons by a relativistic plasma wave excited by a two-frequency laser beam has been demonstrated. No electrons were observed when none were injected or when the laser was operated on a single frequency. However, electrons up to the detection limit of 9.1 MeV were observed when 2.1-MeV electrons were injected in a plasma wave excited (over a narrow range of static gas pressures close to the resonance) by a dual-frequency laser beam. The accelerated electron signal was found to be correlated with indirect measurements of the amplitude of the

plasma wave using Thomson and Raman scattering. The energy gain of the electrons suggests plasma-wave amplitudes of at least 8% over a 10-mm interaction length. Thomson scattering measurements indicate plasma-wave amplitudes up to (15-30)%, offering the possibility of measuring even greater energy gains in future experiments.

The authors would like to acknowledge useful discussions with Dr. W. B. Mori and Dr. P. Mora and Professor J. M. Dawson and Professor T. Katsouleas and thank M. T. Shu and D. Gordon for their technical assistance. This work was supported by the U.S. Department of Energy under Contracts No. DE-AS03-83-ER40120 and No. DE-FG03-92-ER40727.

^(a)Present address: Lawrence Berkeley Laboratory, Berkeley, CA 94720.

^(b)Present address: Florida A&M University, Tallahassee, FL 32307.

- [1] J. M. Dawson, *Sci. Am.* **260**, No. 3, 54 (1989).
- [2] C. Joshi *et al.*, *Nature (London)* **311**, 525 (1984); T. Tajima and J. M. Dawson, *Phys. Rev. Lett.* **43**, 267 (1979); B. I. Cohen *et al.*, *Phys. Rev. Lett.* **29**, 581 (1972); C. M. Tang *et al.*, *Appl. Phys. Lett.* **45**, 375 (1984).
- [3] C. E. Clayton *et al.*, *Phys. Rev. Lett.* **54**, 2343 (1985); N. A. Ebrahim, *Phys. Canada* **45**, 178 (1989).
- [4] Y. Kitagawa *et al.*, *Phys. Rev. Lett.* **68**, 48 (1992).
- [5] A. E. Dangor *et al.*, *Phys. Scr.* **T30**, 107 (1990); F. Amironov *et al.*, *Phys. Rev. Lett.* **68**, 3710 (1992).
- [6] C. E. Clayton *et al.* (to be published).
- [7] W. P. Leemans *et al.*, *Phys. Rev. Lett.* **68**, 321 (1992); J. P. Matt *et al.*, *IEEE Trans. Plasma Sci.* **15**, 173 (1987).
- [8] C. E. Clayton and K. A. Marsh, *Rev. Sci. Instrum.* (to be published).
- [9] C. Joshi *et al.*, in *Proceedings of the Workshop on Advanced Accelerator Concepts*, Port Jefferson, edited by J. Wurtele (AIP, New York, to be published).
- [10] C. Darrow *et al.*, *Phys. Rev. Lett.* **56**, 2629 (1985).
- [11] W. P. Leemans *et al.*, *Phys. Rev. Lett.* **67**, 1434 (1991).
- [12] C. E. Clayton *et al.*, *Phys. Rev. Lett.* **51**, 1656 (1983).
- [13] D. W. Forslund *et al.*, *Phys. Rev. Lett.* **54**, 558 (1985).
- [14] C. Joshi *et al.*, *Phys. Rev. Lett.* **47**, 1285 (1981).
- [15] W. Leemans *et al.*, *Phys. Rev. A* **46**, 1091 (1992); W. P. Leemans *et al.*, in *Proceedings of the IEEE Particle Accelerator Conference, San Francisco, 1991* (IEEE, New York, 1991), p. 2560.
- [16] D. Umstadter *et al.*, *Phys. Rev. Lett.* **59**, 292 (1987).
- [17] M. Rosenbluth and C. S. Liu, *Phys. Rev. Lett.* **29**, 707 (1972).
- [18] R. Williams *et al.*, *Laser Part. Beams* **8**, 427 (1990).
- [19] P. Mora, *Phys. Fluids* **84**, 1630 (1992).

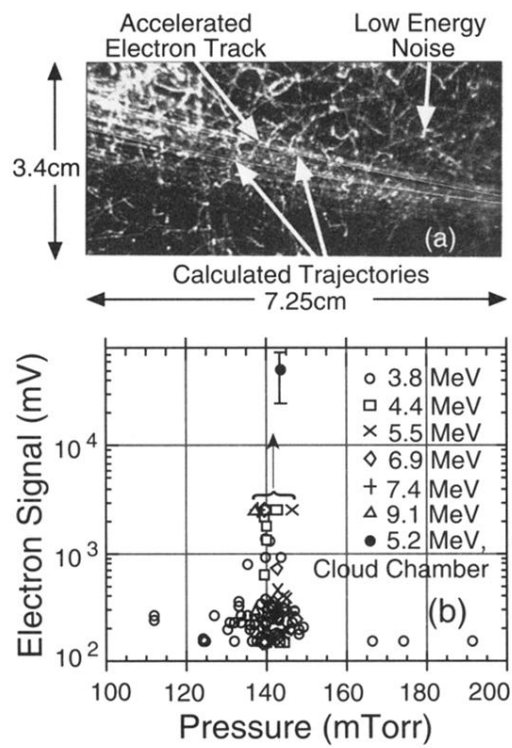


FIG. 2. (a) Electron trajectories in the cloud chamber with the magnetic field. The entrance aperture is located 6 cm to the right of this image. The superimposed curves represent theoretical trajectories for 5.2-MeV electrons. (b) Summary plot showing the electron signal on SBD obtained at various energies vs fill pressure. The one solid symbol is from cloud chamber data converted into units of equivalent SBD signal in mV. The mean noise level [9] was about 150 mV.

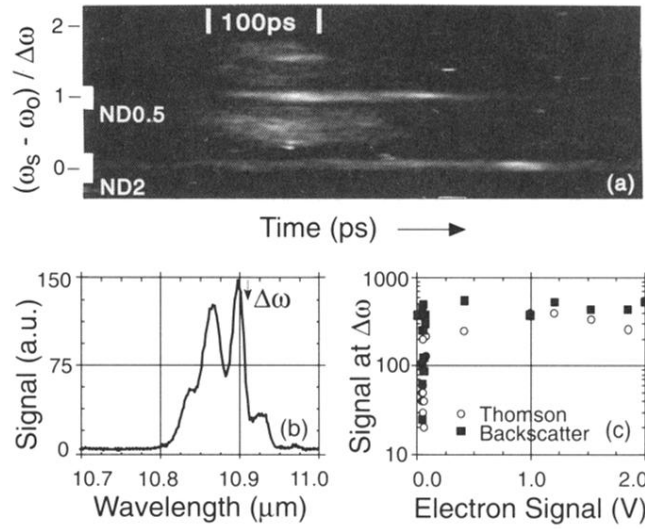


FIG. 3. (a) A streak image showing the time evolution of the Thomson scattered spectrum from modes near $2k_1$. The white boxes on the left indicate the location of neutral density attenuators to limit the signal at zero frequency shift (stray light and scattering from SBS ion wave) and at the plasma-wave frequency. (b) Typical data from the time-integrated backscatter spectrometer. The arrow shows the location for an exact $\Delta\omega$ shift of the 10.59- μm pump. (c) Correlation of the intensity of the first burst of Thomson scattered light at $(\omega_s - \omega_0)/\Delta\omega = 1$ and the backscattered light near $\Delta\omega(10.9 \mu\text{m})$ vs SBD electron signal for one set of data.